ChemCatChem

Research Article
doi.org/10.1002/cctc.202300555

Chemistry Europe
European Chemical Societies Publishing

www.chemcatchem.org

An Eco-Friendly and Switchable Carbon-Based Catalyst for Protection-Deprotection of Vicinal Diols

Inmaculada Román,[a] Rosario Pardo-Botello,*[a] Carlos J. Durán-Valle,[a] Pedro Cintas,[a] and R. Fernando Martínez*[a]

Even though protection-free protocols represent a key principle of green chemistry, both protection and deprotection routes are indispensable strategies in synthetic pursuits, especially towards highly functionalized pharmaceuticals and agrochemicals, often decorated by promiscuous OH or NH groups, among others. Herein a sustainable carbon-based catalyst is reported that efficiently promotes the protection of 1,2-diols as isopropylidene ketals under heterogeneous conditions, affording products in high conversion and yields. Grafting of sulfonate groups onto the high-surface-area carbon creates a solid acid catalyst with high performance for acetalization under mild thermal conditions. Interestingly, the same catalyst can be employed for the inverse deprotection step leading to the parent diols with comparable efficiency. Along with a detailed catalyst's characterization, critical issues related to catalyst loading, reaction scope, and selectivity were thoroughly optimized. The catalyst can be recycled, and no impurities caused by leaching could be observed.

Introduction

Carbon-based catalysts are receiving considerable attention in recent years as highly active and reusable low-cost materials for multiple synthetic applications. Although carbonaceous materials can be generated from numerous organics after thermal treatment, they can also be prepared from inexpensive and renewable biomass and subsequently grafted with appropriate functional groups aimed at specific applications.[1–4] Such heterogeneous catalysts are progressively replacing homogeneous catalysts that exhibit undesirable side effects, such as corrosion derived from acid/basic wastes and they are also difficult to separate and recycle.[5] Still, heterogeneous catalysis should face some challenging drawbacks associated to high loading, low catalytic performance, poor reusability, or high temperature for catalysis to occur. It is well known that, within the realm of sustainable organic synthesis, numerous reactions, taken as fundamental pillars for granted, exhibit poor to modest efficiency in terms of green metrics and energy-mass integration, leaving aside safety issues of importance.[6] Simplification is clearly a strategy that improves process metrics and maximizes resource efficiency. Yet, some operational multistep protocols are compulsory, a point well portrayed by protection-deprotection, which allows site chemoselectivity and often adds functionality to a molecule.[7] Without this toolbox, complex structures like natural products or active pharmaceutical ingredients (APIs) would be virtually inaccessible. Thus, construction of nucleoside antivirals requires the selective protection of contiguous OH groups, usually via acetalization, prior to selective functionalization, as exemplified by recent, short non-enzymatic syntheses of Molnupiravir against SARS-CoV-2 virus.[8,9] And conversion of glycerol to solketal, a renewable fuel additive, also benefits from acetalization using a metal-free solid catalyst.[10] Herein we describe the facile preparation of a robust HSO_3-doped activated charcoal working as dual catalyst for both protection of vicinal 1,2-diols and ketal unlocking. Reaction conditions and product isolation involves minimal impact caused by washes, wastes, along with chromatographic and carbon cleanups. In fact, the transformation is essentially chromatography-free; even products once described as oily substances could now be obtained as stable and less hazardous crystalline materials. Sulfonated activated carbon has proven to be a versatile heterogeneous catalyst, and previous studies show applications, among others, to the synthesis of *N*-alkyl imidazoles and imidazolium ionic liquids,[11] substituted quinolines,[12] benzodiazepine derivatives,[13] biodiesel production,[14,15] and hydrolysis reactions.[16–18]

[a] *I. Román, Dr. R. Pardo-Botello, Prof. Dr. C. J. Durán-Valle, Dr. P. Cintas, Dr. R. Fernando Martínez*
Departamento de Química Orgánica e Inorgánica, Facultad de Ciencias, and Instituto Universitario de Investigación del Agua, Cambio Climático y Sostenibilidad, (IACYS)
Universidad de Extremadura
Avenida de Elvas s/n, 06006-Badajoz (Spain)
E-mail: rmarvaz@unex.es
rpardo@unex.es

Supporting information for this article is available on the WWW under https://doi.org/10.1002/cctc.202300555

Results and Discussion

Synthesis and characterization of catalysts

Norit RX3 (hereafter referred to as **N**), belonging to the Norit-type family of activated carbons (Cabot Corporation) was used as precursor for the preparation of two different activated carbonaceous catalysts (see the Supporting Information for Experimental Section). Sulfonated Norit (**NS**) was prepared by treating **N** with concentrated sulfuric acid for 90 min at room temperature. Likewise, commercial **N** was oxidized with

concentrated nitric acid for 90 min at room temperature to give the catalyst **NN**.

The parent charcoal **N**, as well as its derivatives **NS** and **NN**, displayed type 4 adsorption-desorption isotherms at 77 K,[19] since hysteresis loops were observed. This shows that the three catalysts mainly possess a microporous structure with a certain volume of mesopores (Figure 1). Treatment with concentrated sulfuric acid led to a lower adsorption of N_2, whereas treatment with nitric acid slightly increases the adsorption capacity, although both catalysts gave similar results compared to the starting material **N**.

Furthermore, H4 loops for **N**, **NS** and **NN** could be identified, which are closed at relative pressure values of approximately 1. These results suggest the lack of cylinder-shaped pores and the presence of slit-shaped mesopores.

Table 1 collects specific surfaces found for **N**, **NS** and **NN** by applying the Brunauer-Emmet-Teller model (BET) to the data of the isotherms shown in Figure 1. As expected from such adsorption isotherm data, specific surfaces do not vary significantly after the treatment with sulfuric or nitric acid.

Table 2 gathers data corresponding to the elemental analysis of **N**, **NS** and **NN**, where the percentage of oxygen was calculated by difference.

The main constituent of all these catalysts is obviously carbon. The treatment of **N** with sulfuric acid led to a charcoal with a similar composition, except the sulfur content, which increases considerably after the aforementioned protocol. Similarly, the treatment of parent charcoal **N** with nitric acid led to a material with more nitrogen content.

XPS data are compiled in Table 3, Table S1, Figure 2 and Figure S1. Catalyst oxidation is observed after treatment with acids. There are no significant changes in the nitrogen composition of the catalysts whilst the sulfur content is increased after the treatment with sulfuric acid. The amount of heteroatoms is higher than that found by elemental analysis, which implies that the chemical treatment modifies mainly the surface of the catalysts.

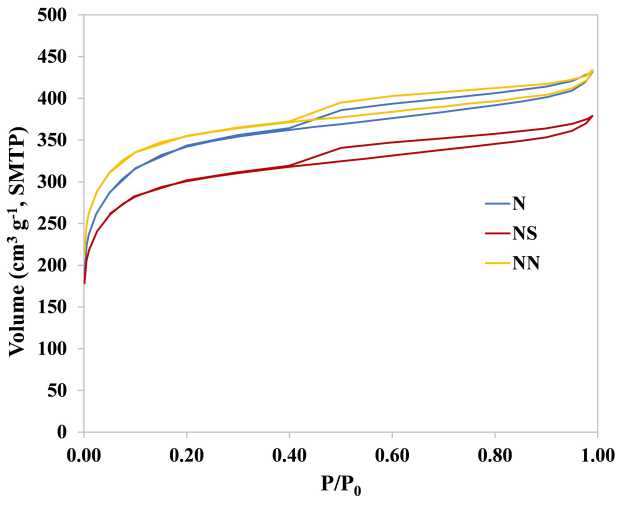

Figure 1. N_2 adsorption isotherms of **N**, **NS** and **NN**.

Table 1. Specific surfaces of catalysts **N**, **NS** and **NN**.

Catalyst	Specific surface [$m^2 g^{-1}$]
N	1249
NS	1117
NN	1324

Table 2. Elemental analysis of **N**, **NS** and **NN**.

Catalyst	C [%]	H [%]	N [%]	O [%]	S [%]
N	89.1	1.4	0.5	8.5	0.5
NS	89.2	1.0	0.5	8.2	1.1
NN	90.1	0.6	1.0	8.0	0.3

XPS spectra of C1s (Figure 2 and Table S1) show a reduction of component 1 (*ca.* 284.8 eV), corresponding to reduced forms of carbon (aromatic and aliphatic hydrocarbons), and an increasement of component 2 (*ca.* 286 eV), usually assigned to C–O bonds. The third component increases as well. These findings fully agree with catalyst's surface oxidation, as evidenced by measuring elemental compositions.

The main peak of XPS spectra of O 1s is found at *ca.* 531 eV, characteristic of oxygen-containing functional groups. After chemical treatment of the catalyst, another peak could be detected at a higher value of B:E., due to the presence of functional groups more oxidized than the parent carbon.

The most important change is observed in the catalyst **NN**, where the peak for the most reduced form of nitrogen decreases (*ca.* 396 eV) and a new peak is found at higher energy (406.1 eV), which can be assigned to either nitrate or nitro groups arising from the oxidation of the catalyst with nitric acid. The most reduced forms of nitrogen have been apparently oxidized or lixiviated after the above treatment.

Three components are detected in the XPS spectra of S 2p: one at 159 eV that can be assigned to sulfides; another peak is observed at 165 eV, attributable to organic sulfur (like thiols), along with a peak at 170 eV, consistent with the presence oxidized forms of sulfur such as sulfonic and sulfate groups. The last two peaks decrease after treatment with nitric acid, thus suggesting the lixiviation of the aforementioned groups. The most relevant result is the increase in the intensity of the peak at 169 eV for the catalyst **NS** that would confirm the presence of sulfonic groups.

Finally, Table 4 collects PZC measurements, as well as the quantification of acid and basic groups for each solid.

As inferred from the PZC value shown in Table 4, parent charcoal **N** is neutral. This value is lower than usual for this type of materials, which are generally found to be alkaline.

Table 3. XPS analysis for **N**, **NS** and **NN**.

Catalyst	C 1s [%]	O 1s [%]	N 1s [%]	S 2p [%]
N	86.2	10.9	2.6	0.3
NS	82.1	14.3	2.2	1.4
NN	82.3	15.2	2.4	0.1

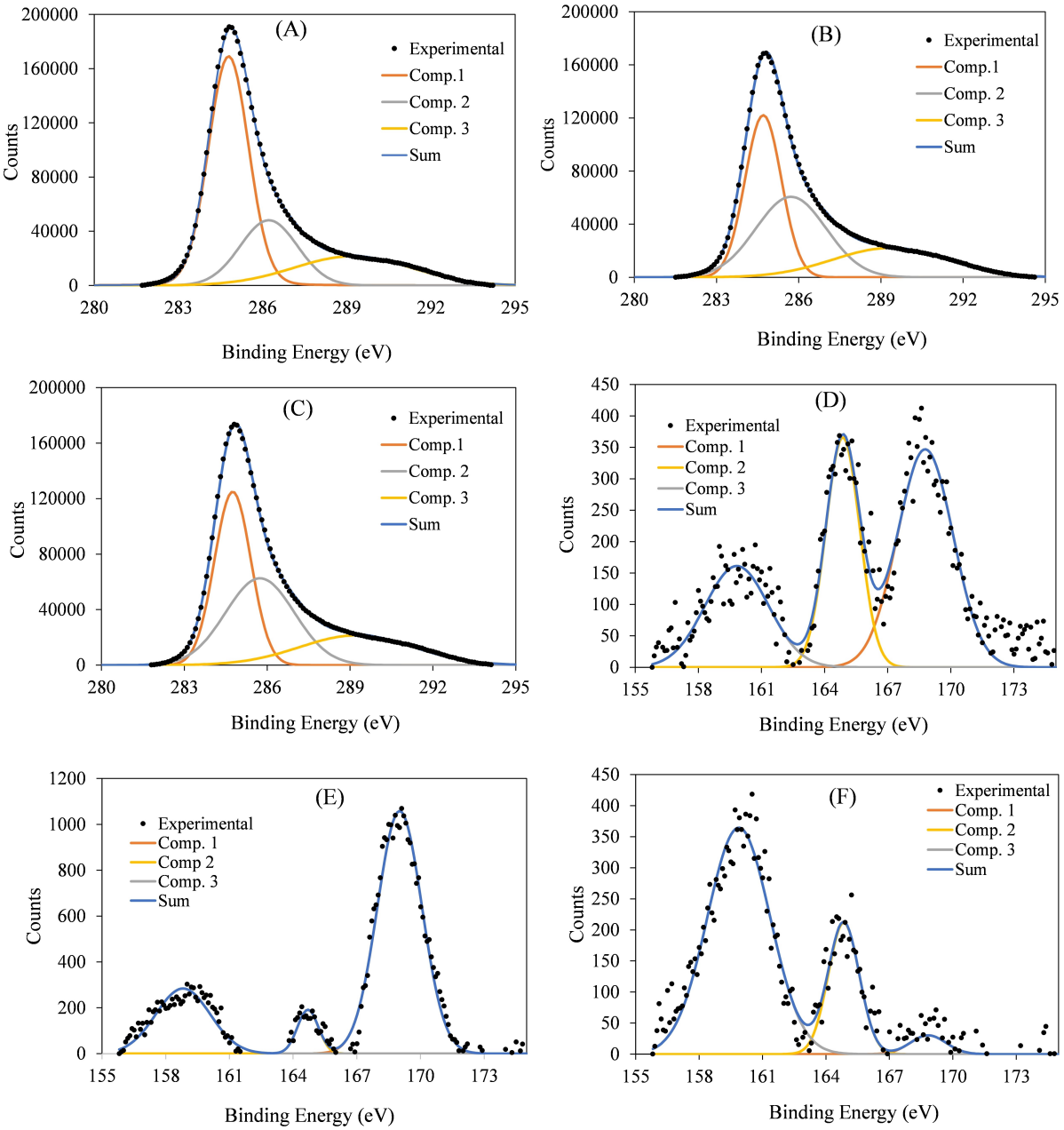

Figure 2. XPS spectra of: (A) catalyst **N** (C 1s); (B) catalyst **NS** (C 1s); (C) catalyst **NN** (C 1s); (D) catalyst **N** (S 2p); (E) catalyst **NS** (S 2p); (F) catalyst **NN** (S 2p).

The treatment of **N** with sulfuric acid leads, as expected, to an increased number of acid groups. However, this result cannot be explained exclusively by the oxidation of the catalyst that indeed happens in the case of the catalyst **NN**, for which the oxidation does increase the number of carboxyl and hydroxyl groups (Figure S2 shows enhanced intensity within the range 3300–3500 cm^{-1}, characteristic of OH stretching bands). Accordingly, the higher acidity of **NS** compared to that of **NN** may be attributed to the presence of sulfonic groups on the surface of the catalyst. FT-IR spectrum of **NS** (Figure S2) shows vibrational bands at 1112 and 617 cm^{-1}, which confirms in addition this assignment.[20]

On the other hand, catalysts **NN** and **NS** possess more acid groups grafted on their surface than basic sites, due to the treatment of the parent charcoal with nitric and sulfuric acid, respectively. To assess whether or not such a grafting had any influence on the surface morphology, scanning electron micro-

Table 4. PZC measurements of catalysts **N**, **NS** and **NN**.

Catalyst	PZC[a]	Acid groups[b]	Basic groups[b]
N	7.1	0.44	0.44
NS	2.8	0.73	0.14
NN	3.8	0.86	0.43

[a] Point of zero charge. [b] Measured as mEq g^{-1}.

scopy (SEM) was performed on the three catalysts and the resulting images (Figure S3) show a similar pattern in all cases.

Acetalization screening of diols under heterogeneous acid catalysis

The preliminary study on the acetalization reaction involved the model diols **1** and **2**, bearing aromatic rings which facilitated TLC monitoring with UV detection. As acetalization agents, propan-2-one (**3**), 2,2-dimethoxypropane (**4**) and 2-methoxypropene (**5**) were used because they are the most common reagents for the preparation of isopropylidene ketals (Scheme 1), while the three catalysts, namely **N**, **NS**, and **NN** were also taken into account.

As stated above, catalysts **NS** and **NN** were found to be acidic enough since the PZC values measured obtained were 2.8 and 3.8, respectively.

Acetalization reactions were performed at 80 °C with magnetic stirring in a sealed vial, to minimize solvent loss and ensure the absence of moisture inside the reaction media. Reactions were monitored and judged to be complete by TLC analysis (Table 5).

As shown in Table 5, the use of propan-2-one (**3**) and 2-methoxypropene (**5**) with a 10% of catalyst **NS** drove to the formation of acetonide **6** in moderate yields (entries 1 and 4). Moreover, in both cases purification by column chromatography was required due to presence of impurities accompanying the crude reaction mixture. However, acetalization reactions of diols **1** and **2** with the same amount of catalyst **NS**, using now 2,2-dimethoxypropane (**4**), led to ketals **6** and **7** with excellent yields (90%) and did not require purification by chromatography (entries 2 and 3).

Protection of diol **1** with 2,2-dimethoxypropane (**4**) took place slowly in the presence of pristine **N** (entries 5–7), as expected for a non-acidic catalyst with a PZC value of 7.1. Obviously, the absence of catalyst gave no reaction (entry 8).

Finally, we also explored the reaction of diol **1** with 2,2-dimethoxypropane (**4**) and the acid catalyst **NN** (entry 9). An excellent yield was obtained under these conditions (92%), even though a longer reaction time was needed for completion compared to the reaction employing the same amount of catalyst **NS** (entry 2). From these results, one can conclude that the optimum conditions for diol acetalization involve the use of catalyst **NS** and 2,2-dimethoxypropane (**4**) as reagent. The structure of acetonides **6** and **7** was confirmed by means of FT-IR (Figures S5–S6) and NMR (Figures S14–S17) spectra.

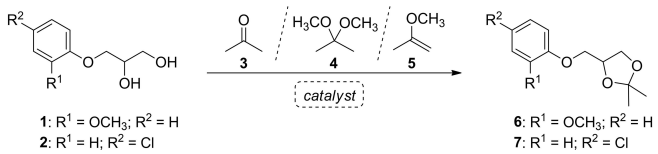

Scheme 1. Initial screening of acetalization.

Table 5. Initial screening of reaction conditions for the acetalization of 1,2-diols.

Entry	Diol	Reagent	Catalyst (%)[a]	Time	Product	Yield [%]
1	**1**	**3**	**NS** (10)	5d	**6**	60[c]
2	**1**	**4**	**NS** (10)	3.5 h	**6**	90[b]
3	**2**	**4**	**NS** (10)	3.5 h	**7**	90[b]
4	**1**	**5**	**NS** (10)	1 h	**6**	70[c]
5	**1**	**4**	**N** (10)	3 h	**6**	0
6	**1**	**4**	**N** (10)	1d	**6**	0
7	**1**	**4**	**N** (10)	8d	**6**	90[b]
8	**1**	**4**	No catalyst	2d	**6**	0
9	**1**	**4**	**NN** (10)	2d	**6**	92[b]

[a] Percentage of catalyst with respect to the starting weight of diol. [b] Isolated yield without purification by column chromatography. [c] Isolated yield after purification by column chromatography.

Remarkably, reactions of diols **1** and **2** with 10% of the catalyst **NS** led to ketals **6** and **7** in high purity. These acetonides, previously reported as oils,[21,22] crystallized on standing after removing the acetalization reagent out of the reaction mixture and, as stated above, without purification by chromatography. Additionally, elemental analysis of both acetonides **6** and **7** were in complete agreement with the calculated values (see Experimental Section, SI).

Catalyst load optimization

Next, we investigated the effect of the catalyst load on the acetalization reactions of diols **1** and **2**. Both 2,2-dimethoxypropane (**4**) and variable loads of the catalyst **NS**, expressed as the percentage with respect to the weight of starting material: 20%, 10%, 5%, and 2%, were used (Table 6).

Table 6 shows very good yields for all the experiments, over 89% in all cases. The use of either 20% or 10% of catalyst **NS** gave rise to isolated yields about 90% (entries 1–4). The reduction of the catalyst load led to the formation of acetonides **6** and **7** in excellent yields (entries 5–8). These results suggest that the adsorption of the diol onto the catalyst surface is favored as the catalyst load increases, which is consequently detrimental to the yield of this reaction. By taking into account these findings, 5% of catalyst loading was preferred over the 2%-figure, as the former would minimize any weighing error.

Table 6. Catalyst load optimization.

Entry	Diol	**NS** [%][a]	Time [h]	Yield [%][b]
1	**1**	20	2.5	92
2	**2**	20	2	89
3	**1**	10	3.5	90
4	**2**	10	3.5	90
5	**1**	5	3	94
6	**2**	5	2	94
7	**1**	2	3	95
8	**2**	2	4	97

[a] Percentage of catalyst with respect to the starting weight of diol. [b] Isolated yield without purification by column chromatography.

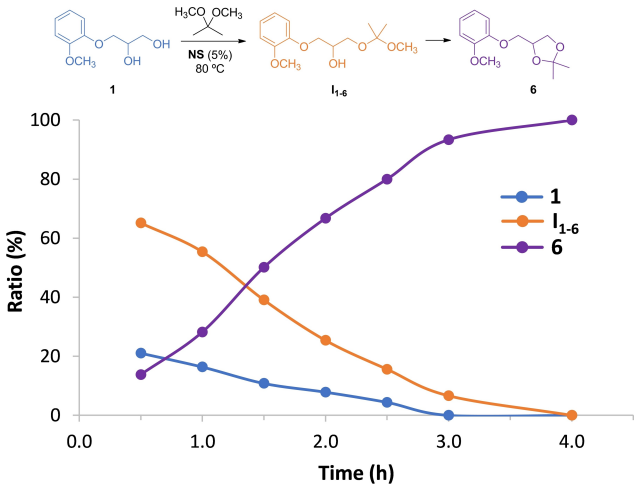

Figure 3. Effect of the reaction time on the acetalization of diol **1**.

In order to rule out the catalytic effect caused by a potential leaching of the catalyst **NS**, we also performed an experiment that consisted in filtering the catalyst (5% wt) before the reaction of diol **1** to form acetonide **6** goes to completion (Figure S4). Thus, the catalyst was removed after 2.5 h, and the resulting filtrate was again heated at 80 °C, and monitored by TLC and ^{1}H NMR. The composition of the reaction mixture did not change within the following 24 h, thereby evidencing that the actual catalysis is promoted by the solid catalyst **NS**.

Furthermore, the effect of the reaction time on the acetalization of diol **1** leading to compound **6** was studied as well, by using again 5% of catalyst **NS**. As shown in Figure 3, diol **1** is rapidly transformed into the intermediate $\mathbf{I}_{1-6}$, from which acetonide **6** arises almost quantitatively after 3 h.

Reaction scope

Once the conditions for the acetalization of diols **1** and **2** were optimized with 2,2-dimethoxypropane (**4**) and 5% of the catalyst **NS**, the next goal was to explore the reaction scope with other commercially available diols. For this study diols bearing aromatic (**8**), heterocyclic (**9**), and heteroaromatic rings (**10** and **11**), along with alkyl groups (**12** and **13**) were included. We also considered the symmetrically-substituted polyol **14** derived from glycerol (Scheme 2).

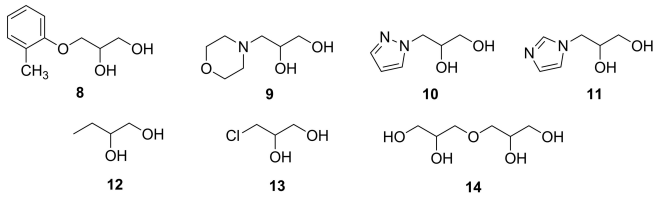

Scheme 2. Substrates employed in the acetalization reaction.

Table 7. Reaction scope.

Entry	Diol	NS [%][a]	Time	Product	Yield [%][b]
1	**8**	5	2 h	**15**	94
2	**9**	5	24 h	**16**	NR[c]
3	**10**	5	5 h	**17**	91
4	**11**	5	24 h	**18**	NR[c]
5	**12**	5	4.5 h	**19**	90
6	**13**	5	4.5 h	**20**	89
7	**14**	5	2 h	**21**	99[d]

[a] Percentage of catalyst with respect to the starting weight of diol. [b] Isolated yield without purification by column chromatography. [c] No reaction under these conditions. [d] Isolated yield as a mixture of isomers (see below).

Data compiled in Table 7 show the reaction could be successfully applied to diols **8**, **10**, **12**, **13**, and polyol **14**. In these cases, the isolated yields for the corresponding acetonides were excellent (>89%, entries 1, 3, 5, 6 and 7). However, the reaction did not take place with diols **9** and **11** (entries 2 and 4). Such diols possess nitrogen atoms, which are basic enough to be protonated by the acid catalyst **NS** ($pK_a = 8.5$ for morpholine; $pK_a = 6,9$ for imidazole), thereby losing its catalytic activity. This limitation, however, does not occur for diol **10** derived from pyrazole, having a much lower pK_a and accordingly a less basic behavior than the above-mentioned diols (Scheme 3).[23,24]

Structural elucidation of the acetonides could easily be inferred from ^{1}H and ^{13}C NMR spectra (Table S2, Figures S18–S27). All compounds showed typical signals attributed to the isopropylidene group. Two singlets were identified in the ^{1}H NMR spectra, corresponding to the methyl hydrogens at the 1,3-dioxolane ring. The ^{13}C shifts at ~109 ppm were assigned to the quaternary carbon of the isopropylidene group, whereas methyl carbons resonated between 27.0 and 25.4 ppm.

Acetalization reaction of polyol **14**, commercially available in 80% purity as mixture of isomers, led to a mixture of two products where the diacetonide **21** was found to be the major component (Scheme 4). Purification by column chromatography

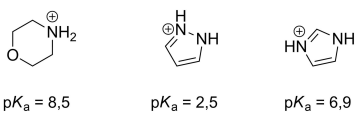

Scheme 3. pK_a values for morpholine, pyrazole and imidazole.[23,24]

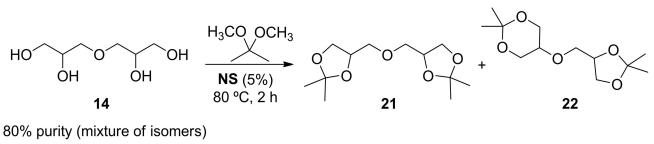

Scheme 4. Acetalization reaction of polyol **14**.

gave rise to pure **21** (74% yield) together with a 1:1 mixture of **21** plus another isomer, for which the structure of **22** was proposed (25% yield).

The structure of **21** and **22** was confirmed by NMR. ^{1}H NMR spectrum of **21** displayed signals corresponding to two isopropylidene groups belonging to a symmetrical structure, as evidenced by two singlets at 1.42 and 1.36 ppm (Figure S26). Likewise, ^{13}C NMR spectrum shows two signals at 26.9 and 25.5 ppm, assigned to the carbons of the same methyl groups, and a peak at 109.5 ppm due to the quaternary carbon (Figure S27). We could confirm the structure of **22** from the NMR spectra of the 1:1 mixture containing **21** and its isomer **22**. The presence of a 1,3-dioxane ring was corroborated by signals corresponding to 10 hydrogen atoms between 4.31 and 3.49 ppm, the signal of the quaternary carbon at 98.4 ppm, and four signals assigned to methylene carbons at 70.2, 66.9, 62.8, and 62.6 ppm (Figures S28 and S29).

Finally, acetalization of D-mannitol (**23**), a naturally occurring polyol, widely used as additive in pharmaceutical and food industries, was also attempted. In this case, 10% of catalyst **NS** was needed for completion. After 3 hours, a major compound was detected by TLC (R_f = 0.3, hexane/ethyl acetate, 1:1). The reaction mixture was then filtered, and the solvent removed under reduced pressure to give diol **24** as a white solid in 77% yield (Scheme 5).

Interpretation of ^{1}H and ^{13}C NMR spectra allowed us to corroborate the structure of **24**. The existence of a symmetry center led to simpler NMR spectra. Thus, the peak at 4.70 ppm is due to the hydroxyl group. Between 4.03 and 3.43 ppm the signals assigned to the hydrogen atoms of CH and CH_2 groups are observed, whereas the methyl group hydrogens resonate at 1.29 and 1.25 ppm (Figure S30). On the other hand, the quaternary carbon of the isopropylidene group is detected at 108.1 ppm, the chemical shifts for the CH and CH_2 groups within the range 74.8–66.7 ppm, and the methyl group carbons appear at 26.9 and 25.5 ppm (Figure S31). FT-IR spectrum showed broad bands attributed to the hydroxy groups at 3391 and 3273 cm^{-1} (Figure S12).

In a different experiment, the reaction of D-mannitol with 2,2-dimethoxypropane and 10% of catalyst **NS** was heated at 80 °C for a longer time, with the aim of achieving the total protection of the polyol. Thus, the reaction was essentially complete after 2 days, and triacetonide **25** could be isolated in excellent yield (94%) as a yellowish solid (Scheme 6).

Again, NMR spectra of **25** confirmed the presence of three isopropylidene groups belonging to a symmetric structure as well. The ^{1}H NMR spectrum showed three singlets at 1.43, 1.39, and 1.36 ppm, assigned to the methyl hydrogens (Figure S32). The ^{13}C NMR spectrum (Figure S33) displayed two peaks corresponding to quaternary carbons (110.3 and 109.7 ppm) and three signals due to methyl carbons (27.6, 26.7 and 25.5 ppm). Moreover, FT-IR spectrum confirmed the lack of the stretching bands characteristic of the hydroxyl group (Figure S13).

Catalyst recyclability

The acetalization reaction of diol **1** was selected to study the recyclability of the catalyst **NS**. Thus, such a diol was transformed into acetonide **6** under the optimized conditions previously described (80 °C, 5% of catalyst **NS**, 2,2-dimethoxypropane), starting from a 2-gram scale of diol **1**. For each run, the reaction was monitored again by TLC analysis. After completion, the catalyst was filtered and dried at 140 °C overnight. Such a catalyst was directly used for the following run without any regeneration treatment, under the same reaction conditions.

As collected in Table S3, the isolated yields were excellent after 3 runs ($\geq$90%). Nevertheless, the catalytic capacity of **NS** decreased as the catalyst was reused. Thus, the third run led to an excellent yield (99%), even though 4 days were needed for achieving completion.

Hydrolysis of acetonides under acid catalysis

In order to check the versatility of the catalytic system, we explored the hydrolysis of acetonides **6** and **7** by using the same catalyst employed in their formation, i.e. catalyst **NS**. We thought this double protection-deprotection function would enhance the sustainability of the carbonaceous catalyst, since it could be used for both the protection of a given diol and the hydrolysis of the synthesized acetonide. This would likewise be highly beneficial (in terms of atom economy and waste reduction) for a synthetic route where acetonide protection was needed. The hydrolysis reaction was conducted in a 1:1 mixture of 1,4-dioxane (as solubilizing agent) and water, and were

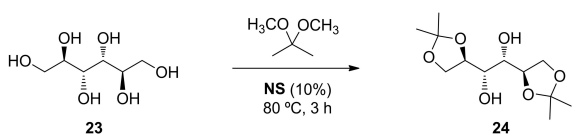

Scheme 5. Selective acetalization reaction of D-mannitol **23** to give **24**.

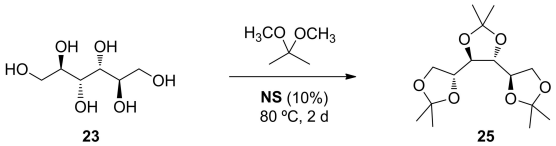

Scheme 6. Acetalization reaction of D-mannitol **23** to give **25**.

Table 8. Deprotection reaction of acetonides **6** and **7**.

Entry	Substrate	**NS** [%][a]	Time [h]	T [°C]	Yield [%]
1	**6**	10	48	rt	NR[b]
2	**6**	10	4	80	90[c]
3	**7**	10	4	80	87[c]
4	**6**	5	5	80	90[c]
5	**7**	5	24	80	88[c]

[a] Percentage of catalyst with respect to the starting weight of substrate. [b] No reaction under these conditions. [c] Isolated yield without purification by column chromatography.

monitored, as usual, by TLC until complete consumption of starting material (Table 8).

As shown in Table 8, the reaction did not take place at room temperature (entry 1). At 80 °C, however, deprotection reactions worked well as inferred from TLC analyses. The reduction of the catalyst loading from 10% to 5% led to almost identical yields (90%–87%, entries 2–5), but reaction times took longer, especially for the reaction of acetonide **7**.

In view of these results, we next carried out the deprotection of acetonides **15**, **17**, **19**, **20** and **21** under the same conditions (Table 9).

Hydrolysis reactions proceeded with very good yields (> 84%) for acetonides **15**, **17** and **21** (entries 1, 2 and 5). Substrates **19** and **20**, however, were transformed into their corresponding diols in slightly lower yields (79% for **12** and 81% for **13**), probably due to the high volatility of the starting acetonides.[25,26] It should be noted that neither of them required any further purification step by chromatography. In all cases, ^{1}H NMR spectra of the hydrolyzed compounds evidenced the absence of signals attributable to isopropylidene groups.

Green assessment

Achieving sustainability cannot solely be related to the qualitative use of the 12 principles of green chemistry (partially, at least), but to a portfolio of quantitative metrics. To this end, Tables 10 and 11 show a comparative and critical analysis of both protection and deprotection reactions, using a series of well-representative metrics, namely atom economy (AE), reaction mass efficiency (RME), mass intensity (MI), and mass productivity (MP).[27] While isolated yields range from good to excellent, atom economy data disclose a more realistic view of efficiency as reactions are run at stoichiometric excess of one reactant. The release of two methanol molecules per diol unit in protection reactions account for modest RME figures, even if this waste can be distilled and recycled. This is substantially mitigated in deprotection reaction furnishing one equivalent of acetone as carbon footprint, thereby increasing mass efficiency. The amount of catalyst (between 5 and 10 wt%) was deliberately excluded in all metrics, as it could be reused up to three times without substantial loss of catalytic activity.

Table 9. Deprotection reaction of acetonides **15**, **17**, **19**, **20** and **21**.

Entry	Substrate	**NS** [%][a]	Time [h]	Product	Yield [%]
1	**15**	10	4	**8**	91
2	**17**	10	4	**10**	84
3	**19**	10	4	**12**	79
4	**20**	10	4	**13**	81
5	**21**	10	4	**14**	88

[a] Percentage of catalyst with respect to the starting weight of substrate.

Table 10. Green metrics for protection reaction of **1**, **2**, **8**, **10**, **12**, **13** and **14**.

Reaction	Yield [%]	AE [%][a]	RME [%][a]	MI[a]	MP [%][a]
1→**6**	94	78.8	11.9	8.4	11.9
2→**7**	94	79.1	12.0	8.3	12.0
8→**15**	94	77.6	12.2	8.2	12.2
10→**17**	91	74.0	12.4	8.1	12.4
12→**19**	90	67.0	14.1	7.1	14.1
13→**20**	89	70.1	13.1	7.6	13.1
14→**21**	99	65.8	12.6	8.0	12.6

[a] Excluding the substoichiometric amount of catalyst.

Because RME accounts for all mass employed in a given reaction (excluding water), and includes yield, stoichiometry, and AE, that metric has probably become the most useful parameter, especially for assessing the elaboration of APIs (active pharmaceutical ingredients), often proceeding with low AEs and poor mass efficiencies.[28] Water is likewise excluded from mass intensity (MP) estimations, in the present case for deprotection reactions conducted in aqueous dioxane. MI is usually regarded as the metric of choice to evaluate greenness in fine chemistry,[29] because this adimensional ratio (all masses vs mass product) is what one would expect for the *E* factor. The latter is higher in fine chemistry (~20–22) than our data gathered in Tables 10 and 11.

Mass productivity (MP), being the reciprocal of MI, is a thoughtful metric for business, as it highlights resource utilization.[29] Clearly, MP is usually *uncomfortable* in green synthesis, as the low values in multistep procedures (~1–5%) means that the major portion of mass used to make products is wasted. Data obtained herein (last column) reflect high overall efficiencies. Moreover, the fact that protection/deprotection can be performed in a circular way using the same catalyst does increase greenness as well.

Table 11. Green metrics for deprotection reaction of **6**, **7**, **15**, **17**, **19**, **20** and **21**.

Reaction	Yield [%]	AE [%][a]	RME [%][a]	MI[a]	MP [%][a]
6→**1**	90	83.2	74.8	6.8	14.8
7→**2**	87	83.5	72.6	7.0	14.2
15→**8**	91	82.0	74.4	9.0	11.1
17→**10**	84	78.0	65.8	11.2	9.0
19→**12**	79	69.2	55.0	11.4	8.8
20→**13**	81	73.4	59.7	10.4	9.6
21→**14**	88	67.5	59.3	17.9	5.6

[a] Excluding the substoichiometric amount of catalyst.

Conclusion

This paper describes a convenient and eco-friendly method for the formation and hydrolysis of acetonides under heterogeneous acid catalysis. The sulfonated catalyst **NS** exhibits superior activity compared to that shown by **NN**. The optimum conditions for the solvent-free acetalization reaction consists in heating the substrate at 80 °C, in a sealed vial, along with 2,2-dimethoxypropane and 5% of the catalyst **NS**. This reaction is applicable to a broad range of diols and other polyols such as D-mannitol, affording products in very good yields (77%–94%) in all cases. The high purity of the resulting acetonides could be corroborated by NMR and elemental analysis. In addition, some acetonides crystallize spontaneously on standing after filtration and removal of the acetalization reagent, thus avoiding further purification protocols (i.e. chromatography), even if some derivatives are reported as oils in the literature. The catalyst **NS** may be reused up to three cycles maintaining excellent yields and without any regeneration treatment. On the other hand, catalyst **NS** is also suitable for the hydrolysis of a series of acetonides, providing good yields (>79%) even for volatile substrates and without additional purification. It is worth highlighting that selectivity was complete for both acetalization and hydrolysis reactions. Therefore, this dual, efficient, metal-free, economical, water-tolerant carbonaceous catalyst has sufficient potentiality for conducting facile acetalization and deacetalization of 1,2-diols. Overall, these aspects examined under batch conditions, should be of interest to be implemented in flow-based protocols and large-scale operations.

Acknowledgements

Financial support from the Junta de Extremadura and Fondo Europeo de Desarrollo Regional (grants IB20026, GR21039 and GR21107) is warmly appreciated.

Conflict of Interests

The authors declare no conflict of interest.

Data Availability Statement

The data that support the findings of this study are available from the corresponding author upon reasonable request.

Keywords: activated charcoal · heterogeneous catalysis · ketalization · protecting groups · sustainable materials

[1] X. Lin, Y. Liang, Z. Lu, H. Lou, X. Zhang, S. Liu, B. Zheng, R. Liu, R. Fu, D. Wu, *ACS Sustainable Chem. Eng.* **2017**, *5*, 8535–8540.
[2] B. Zhang, Y. Jiang, R. Balasubramanian, *J. Mater. Chem. A* **2021**, *9*, 24759–24802.
[3] Z. Chen, X. Zeng, S. Wang, A. Cheng, Y. Zhang, *ChemSusChem* **2022**, *15*, e202200411.
[4] T. Tan, W. Wang, K. Zhang, Z. Zhan, W. Deng, Q. Zhang, Y. Wang, *ChemSusChem* **2022**, *15*, e202201174.
[5] G. Ginnakakis, S. Mitchell, J. Pérez-Ramírez, *Trends Chem.* **2022**, *4*, 264–276.
[6] C. Jiménez-González, D. J. C. Constable, *Green Chemistry and Engineering. A Practical Design Approach*, John Wiley & Sons, Inc., New York, **2011**.
[7] P. G. M. Wuts, in *Greene's Protective Groups in Organic Synthesis, 5th Edition*, John Wiley & Sons, Inc., New York, **2014**, Ch. 2, pp. 17–471 (for protection of hydroxy groups, including 1,2 and 1,3-diols).
[8] V. Gopalsamuthiram, A. L. Kadam, J. K. Noble, D. R. Snead, C. Williams, T. F. Jamison, C. Senanayake, A. K. Yadaw, S. Roy, G. Sirasani, B. F. Gupton, J. Burns, D. W. Cook, R. W. Stringham, S. Ahmad, R. Krack, *Org. Process Res. Dev.* **2021**, *25*, 2679–2685.
[9] T. Hu, Y. Xie, F. Zhu, X. Gong, Y. Liu, H. Xue, H. A. Aisa, J. Shen, *Org. Process Res. Dev.* **2022**, *26*, 358–364.
[10] B. Saini, A. P. Tathod, S. K. Saxena, S. Arumugam, N. Viswanadham, *ACS Sustainable Chem. Eng.* **2022**, *10*, 1172–1181.
[11] C. J. Durán-Valle, M. Madrigal-Martínez, M. Martínez-Gallego, I. M. Fonseca, I. Matos, A. M. Botelho Do Rego, *Catal. Today* **2012**, *187*, 108–114.
[12] J. López-Sanz, E. Pérez-Mayoral, E. Soriano, D. Omenat-Morán, C. J. Durán, R. M. Martín-Aranda, I. Matos, I. Fonseca, *ChemCatChem* **2013**, *5*, 3736–3742.
[13] M. Godino-Ojer, I. Matos, M. Bernardo, R. Carvalho, O. S. G. P. Soares, C. Durán-Valle, I. M. Fonseca, E. Pérez-Mayoral, *Catal. Today* **2020**, *357*, 64–73.
[14] P. D. Rocha, L. S. Oliveira, A. S. Franca, *Renewable Energy* **2019**, *143*, 1710–1716.
[15] Y. Pi, W. Liu, J. Wang, G. Peng, D. Jiang, R. Guo, D. Yin, *Front. Chem.* **2022**, *10*, 944398.
[16] G. S. Foo, A. H. Van Pelt, D. Krötschel, B. F. Sauk, A. K. Rogers, C. R. Jolly, M. M. Yung, C. Sievers, *ACS Sustainable Chem. Eng.* **2015**, *3*, 1934–1942.
[17] L. Qin, T. Ishizaki, N. Takeuchi, K. Takahashi, K. H. Kim, O. L. Li, *ACS Sustainable Chem. Eng.* **2020**, *8*, 5837–5846.
[18] A. Blocher, F. Mayer, P. Schweng, T. M. Tikovits, N. Yousefi, R. T. Woodward, *Mater. Adv.* **2022**, *3*, 6335–6342.
[19] M. Thommes, K. Kaneko, A. V Neimark, J. P. Olivier, F. Rodriguez-Reinoso, J. Rouquerol, K. S. W. Sing, *Pure Appl. Chem.* **2015**, *87*, 1051–1069.
[20] A. R. O. Ferreira, J. Silvestre-Albero, M. E. Maier, N. M. P. S. Ricardo, C. L. Cavalcante, F. M. T. Luna, *J. Mol. Catal.* **2020**, *488*, 110888.
[21] W. L. Nelson, J. E. Wennerstrom, S. R. Sankar, *J. Org. Chem.* **1977**, *42*, 1006–1012.
[22] S. Saha, S. K. Mandal, S. C. Roy, *Tetrahedron Lett.* **2008**, *49*, 5928–5930.
[23] M. Morgenthaler, E. Schweizer, A. Hoffmann-Röder, F. Benini, R. E. Martin, G. Jaeschke, B. Wagner, H. Fischer, S. Bendels, D. Zimmerli, J. Schneider, F. Diederich, M. Kansy, K. Müller, *ChemMedChem* **2007**, *2*, 1100–1115.
[24] M. Lõkov, S. Tshepelevitsh, A. Heering, P. G. Plieger, R. Vianello, I. Leito, *Eur. J. Org. Chem.* **2017**, 4475–4489.
[25] U. Schmidt, J. Talbiersky, F. Bartkowiak, J. Wild, *Angew. Chem. Int. Ed. Engl.* **1980**, *19*, 198–199.
[26] J. Y. He, F. X. Gao, R. M. Hua, *Chin. J. Chem.* **2005**, *23*, 1275–1277.
[27] M. G. T. C. Ribeiro, A. A. S. C. Machado, *Green Chem. Lett. Rev.* **2013**, *6*, 1–18.
[28] C. Jiménez-González, C. S. Ponder, Q. B. Broxterman, J. B. Manley, *Org. Process Res. Dev.* **2011**, *15*, 912–917.
[29] C. Jiménez-González, D. J. C. Constable, C. S. Ponder, *Chem. Soc. Rev.* **2012**, *41*, 1485–1498.

Manuscript received: April 26, 2023
Accepted manuscript online: April 28, 2023
Version of record online: May 19, 2023